$SU(2)$ lattice gluon propagator: Continuum limit, finite-volume effects, and infrared mass scale m_{IR}

V. G. Bornyakov

Institute for High Energy Physics, 142281, Protvino, Russia
and Institute of Theoretical and Experimental Physics, 117259 Moscow, Russia

V. K. Mitrjushkin

Joint Institute for Nuclear Research, 141980 Dubna, Russia
and Institute of Theoretical and Experimental Physics, 117259 Moscow, Russia

M. Müller–Preussker

Humboldt-Universität zu Berlin, Institut für Physik, Newton-Str. 15, 12489 Berlin, Germany

We study the scaling behavior and finite (physical) volume effects as well as the Gribov copy dependence of the $SU(2)$ Landau gauge gluon propagator on the lattice. Our physical lattice sizes range from $(3.0 \text{ fm})^4$ to $(7.3 \text{ fm})^4$. Considering lattices with decreasing lattice spacing but fixed physical volume we confirm (nonperturbative) multiplicative renormalizability and the approach to the *continuum limit* for the renormalized gluon propagator $D_{\mathrm{ren}}(p)$ at momenta $|p| \gtrsim 0.6$ GeV. The finite-volume effects and Gribov copy influence turn out small in this region. On the contrary, in the deeper infrared we found the Gribov copy influence strong and finite-volume effects, which still require special attention. The gluon propagator does not seem to be consistent with a simple polelike behavior $\sim (p^2 + m_g^2)^{-1}$ for momenta $|p| \lesssim 0.6$ GeV. Instead, a Gaussian-type fit works very well in this region. From its width—for a physical volume $(5.0 \text{ fm})^4$- we estimate a corresponding infrared (mass) scale to be $m_{\mathrm{IR}} \sim 0.7$ GeV.

I. INTRODUCTION

The Landau (or Lorenz) gauge gluon and ghost propagators in pure Yang-Mills theories or in full QCD have attracted much interest for many years.

One reason for this interest is that the behavior of these propagators in the infrared (IR) region has been related to gluon and quark confinement [1–3]. In particular, Zwanziger has argued that the gluon propagator should vanish in the IR limit [2,4,5], while the ghost dressing function should become singular.

Another reason for this interest is connected with the importance of the momentum dependence of both propagators, especially in the (deep) IR-region, for the phenomenological analysis of experimental data. Many years ago Parisi and Petronzio [6] have pointed out that nonzero effective gluon mass (or dynamically generated gluon mass) m_g is important to resolve some discrepancies in low-energy tests of QCD, as, e.g., ratios of widths of J/ψ. Since then a number of papers has been dedicated to phenomenological studies of such processes as $J/\psi \rightarrow \gamma X$, $\gamma \rightarrow \pi^0$ transition, nonleptonic B meson decays, etc., where a nonzero value of the effective gluon mass m_g plays a crucial role (for an incomplete list of references see, e.g., the recent papers [7,8]).

Let us note that in order to obtain a reliable value of m_g one needs to know the continuum gluon propagator $D(p)$ in the *deep infrared region*.[1] The definition of the mass m_g is based on the hypothesis of a polelike behavior, i.e. $\sim 1/(p^2 + m_g^2)$, of the gluon propagator at small momenta. In this case the effective gluon mass defines the *infrared mass scale* m_{IR}.

Gauge-variant QCD Green functions may serve also as input to bound state equations as Bethe-Salpeter or Faddeev equations for hadron phenomenology [9–11]. Moreover, at large momenta they should allow a determination of phenomenologically relevant parameters such as $\Lambda_{\overline{MS}}$ or condensates $\langle A^2 \rangle$, $\langle \bar{\psi}\psi \rangle$ by fitting lattice data to continuum expressions obtained from operator product expansion and perturbation theory [12,13] in a certain MOM scheme [14,15].

The search for intertwined asymptotic gluon and ghost propagator solutions of Dyson-Schwinger (DS) and functional renormalization group (FRG) equations showed the existence of infrared solutions exhibiting a powerlike *scaling* behavior [9,16–23]. However, as has been pointed out in [24–27], there are also regular so-called *decoupling* solutions providing an IR-finite limit of both the gluon propagator and the ghost dressing function. In [28] it has been argued, that it seems to be a question of IR boundary conditions posed on the ghost dressing function, what kind

---

[1]Throughout this paper we define the deep infrared region as $|p| \lesssim 0.6$ Gev (see also Sec. VI).

of solution one has to select. It should be noticed that both kinds of solutions can support quark confinement [29].

On the lattice, over the last decade extensive studies of the Landau gauge gluon and ghost propagators have been carried out [30–40]. In the meantime lattice computations have reached lattice volumes even with a linear extension $O(10 \text{ fm})$ in order to discriminate between the above mentioned IR solutions. In this way lattice QCD has been found to support the *decoupling* solution [41–45]. This is true as long as one relies on finite-box periodic boundary conditions and on a gauge condition requiring the Landau gauge functional to take extrema as close as possible to the global extremum.

The Gribov copy influence still remains a serious problem in the lattice calculations, at least, in the deep IR-region. The gauge condition we employ require the Landau gauge functional to take extrema as close as possible to the *global* extremum.[2] This choice is supported by the following facts:

(i) a consistent nonperturbative gauge fixing procedure proposed by Parrinello-Jona-Lasinio and Zwanziger (PJLZ-approach) [50,51] presumes that the choice of a unique representative of the gauge orbit should be through the *global* extremum of the chosen gauge fixing functional;

(ii) in the case of lattice compact $U(1)$ gauge theory in the weak coupling (Coulomb) phase some of the gauge copies produce a photon propagator with a decay behavior inconsistent with the expected zero-mass behavior [52–54]. The choice of the global extremum (see also [55]) permits to avoid such copies and to obtain the physical-massless-photon propagator.

For all practical purposes the system of DS and/or FRG equations has to be truncated. The details of truncation influence the behavior of the Green functions especially in the nonperturbative momentum range around 1 GeV, where the Landau gauge gluon dressing function exhibits a pronounced maximum. Therefore, reliable results from first principles to compare with are highly welcome. On the lattice, for finite volumes such results can be obtained and directly compared with finite-volume DS and FRG results [56,57]. To our knowledge, on the lattice a systematic continuum limit determination of the Landau gluon and ghost propagators for various fixed physical volumes is still missing. Such an evaluation has to make sure that Gribov copy effects, lattice artifacts, and multiplicative renormalizability are sufficiently under control.

Here we present such a study for $SU(2)$ pure gauge theory as a continuation of our investigation in [44]. For gauge fixing we rely on the Landau gauge with a gauge condition requiring the gauge fixing functional to take extrema as close as possible to the global extremum. For

_____

[2]For recent alternative attempts see [46–49].

this aim we employ the simulated annealing algorithm [44,58,59] in combination with nonperiodic $Z(2)$ gauge transformations ("$Z(2)$-flips") [60]. With respect to the latter we search within all $2^4 = 16$ global $Z(2)$ Polyakov loop sectors. We concentrate on the gluon propagator and will present data for three different physical volumes up to $\sim (7.3 \text{ fm})^4$. As done in a preliminary manner in [37] we check for multiplicative renormalizability and provide results for the renormalized propagator and dressing function, respectively, which can be considered already to be continuum ones. In Sec. II we introduce the observables to be computed. In Sec. III some details of the simulation are given, whereas in Sec. IV we discuss the effect of improved gauge fixing. In Sec. V we present our numerical results. Sec. VI is dedicated to the discussion of the deep infrared region and to the definition of an alternative infrared (mass) scale m_{IR}. Conclusions will be drawn in Sec. VII.

II. THE GLUON PROPAGATOR: DEFINITIONS

In order to generate Monte Carlo ensembles of non-gauge-fixed $SU(2)$ gauge field configurations we use the standard plaquette Wilson action

$$S = \beta \sum_x \sum_{\mu > \nu} \left[1 - \frac{1}{2} \text{Tr}(U_{x\mu} U_{x+\mu;\nu} U^\dagger_{x+\nu;\mu} U^\dagger_{x\nu}) \right],$$
$$\beta = 4/g_0^2. \tag{1}$$

g_0 denotes the bare coupling constant, $U_{x\mu} \in SU(2)$ are the link variables. The latter transform under local gauge transformations g_x as follows

$$U_{x\mu} \overset{g}{\mapsto} U^g_{x\mu} = g_x^\dagger U_{x\mu} g_{x+\mu}, \qquad g_x \in SU(2). \tag{2}$$

The standard definition [61] for the dimensionless lattice gauge vector potential $\mathcal{A}_{x+\hat\mu/2,\mu}$ is

$$\mathcal{A}_{x+\hat\mu/2,\mu} = \frac{1}{2i}(U_{x\mu} - U^\dagger_{x\mu}) \equiv A^a_{x+\hat\mu/2,\mu} \frac{\sigma_a}{2}. \tag{3}$$

This definition, which is not unique, can influence the propagator results in the IR region, where the continuum limit is hard to control.

In lattice gauge theory the usual choice of the Landau gauge condition is [61]

$$(\partial \mathcal{A})_x = \sum_{\mu=1}^4 (\mathcal{A}_{x+\hat\mu/2;\mu} - \mathcal{A}_{x-\hat\mu/2;\mu}) = 0, \tag{4}$$

which is equivalent to finding a local extremum of the gauge functional

$$F_U(g) = \frac{1}{4V} \sum_{x\mu} \frac{1}{2} \text{Tr} U^g_{x\mu}, \tag{5}$$

with respect to gauge transformations g_x. $V = L^4$ denotes the lattice volume. The manifold consisting of Gribov copies providing local maxima of the functional (5) and

a semipositive Faddeev-Popov operator is called the *Gribov region* Ω, while that of the global maxima is called the *fundamental modular region* (FMR) $\Lambda \subset \Omega$. Our gauge fixing procedure is aimed to approach Λ.

The (unrenormalized) gluon propagator D and its dressing function Z are then defined (for $p \neq 0$) by

$$D_{\mu\nu}^{ab}(p) = \frac{a^2}{g_0^2}\langle \tilde{A}_\mu^a(k)\tilde{A}_\nu^b(-k)\rangle = \left(\delta_{\mu\nu} - \frac{p_\mu p_\nu}{p^2}\right)\delta^{ab}D(p),$$

(6)

$$Z(p) = D(p)p^2,$$

(7)

where $\tilde{A}(k)$ represents the Fourier transform of the gauge potentials defined by Eq. (3) after having fixed the gauge. a denotes the lattice spacing. The physical momenta p are given by $p_\mu = (2/a)\sin(\pi k_\mu/L)$, $k_\mu \in (-L/2, L/2]$. For $p \neq 0$, one determines $D(p)$ according to Eq. (6)

$$D(p) = \frac{1}{9}\sum_{a=1}^{3}\sum_{\mu=1}^{4}D_{\mu\mu}^{aa}(p),$$

(8)

whereas the "zero-momentum propagator" $D(p = 0)$ is defined as

$$D(0) = \frac{1}{12}\sum_{a=1}^{3}\sum_{\mu=1}^{4}D_{\mu\mu}^{aa}(p = 0).$$

(9)

III. DETAILS OF THE SIMULATION

We have performed Monte Carlo (MC) simulations at various β-values between $\beta = 2.2$ and $\beta = 2.55$ for various lattice sizes L. Consecutive configurations (considered to be statistically independent) were separated by 100 sweeps, each sweep consisting of one local heatbath update followed by $L/2$ microcanonical updates. In Table I we provide the full information about the field ensembles used in this investigation.

TABLE I. Values of β, lattice sizes, number of measurements and number of gauge copies used throughout this paper. Lattice spacing is fixed by taking $\sqrt{\sigma} = 440$ Mev. For the values of the lattice spacing see [62,63] (1 GeV$^{-1} \simeq 0.197$ fm).

β	a^{-1} [GeV]	a [fm]	L	aL [fm]	N_{meas}	N_{copy}
2.20	0.938	0.210	14	2.94	400	48
2.30	1.192	0.165	18	2.97	200	48
2.40	1.654	0.119	26	3.09	200	48
2.50	2.310	0.085	36	3.06	400	80
2.55	2.767	0.071	42	2.98	200	80
2.20	0.938	0.210	24	5.04	400	48
2.30	1.192	0.165	30	4.95	400	48
2.40	1.654	0.119	42	5.00	200	80
2.30	1.192	0.165	44	7.26	200	80

For gauge fixing we employ the $Z(2)$ flip operation as discussed in [60]. For completeness we repeat the main information. The method consists in flipping all link variables $U_{x\mu}$ attached and orthogonal to a $3d$ plane by multiplying them with $-1 \in Z(2)$. Such global flips are equivalent to nonperiodic gauge transformations and represent an exact symmetry of the pure gauge action considered here. The Polyakov loops in the direction of the chosen links and averaged over the $3d$ plane obviously change their sign. Therefore, the flip operations combine the 2^4 distinct gauge orbits (or Polyakov loop sectors) of strictly periodic gauge transformations into one larger gauge orbit.

The second ingredient is the simulated annealing (SA) method, which has been found computationally more efficient than the only use of standard overrelaxation (OR) [59,60,64]. The SA algorithm generates gauge transformations $g(x)$ by MC iterations with a statistical weight proportional to $\exp(4VF_U[g]/T)$. The "temperature" T is an auxiliary parameter which is gradually decreased in order to maximize the gauge functional $F_U[g]$. In the beginning, T has to be chosen sufficiently large in order to allow traversing the configuration space of $g(x)$ fields in large steps. As in Ref. [60] we have chosen $T_{\text{init}} = 1.5$. After each quasiequilibrium sweep, including both heatbath and microcanonical updates, T has been decreased with equal step size. The final SA temperature has been fixed such that during the consecutively applied OR algorithm the violation of the transversality condition

$$\max_{x,a}\left|\sum_{\mu=1}^{4}(A_{x+\hat{\mu}/2;\mu}^a - A_{x-\hat{\mu}/2;\mu}^a)\right| < \epsilon_{\text{lor}}$$

(10)

decreases in a more or less monotonous manner for the majority of gauge fixing trials until the condition (10) becomes satisfied with a unique $\epsilon_{\text{lor}} = 10^{-7}$. A monotonous OR behavior is reasonably satisfied for a final lower SA temperature value $T_{\text{final}} = 0.01$ [64]. The number of temperature steps has been chosen to be 1000 for the smaller lattice sizes and increased to 2000 for the lattice size 30^4 and bigger. The finalizing OR algorithm using the standard Los Alamos type overrelaxation with the parameter value $\omega = 1.7$ requires typically a number of iterations varying from $O(10^2)$ to $O(10^3)$.

In what follows we call the combined algorithm employing SA (with finalizing OR) and $Z(2)$ flips the "FSA" algorithm. By repeated starts of the FSA algorithm we search in each $Z(2)$ Polyakov loop sector several times for the best ("*bc*") copy. The total number of copies per configuration N_{copy} generated for each β-value and lattice size is indicated in Table I. In order to demonstrate the Gribov copy effect we can compare with the results obtained from the randomly chosen first ("*fc*") copy.

Some more details to speed up the gauge fixing procedure are described in [44].

IV. INFLUENCE OF GRIBOV COPIES ON THE GLUON PROPAGATOR

Our efficient gauge fixing procedure changes significantly the momentum dependence of the gluon propagator $D(p)$ in the IR-region in comparison with the result of the standard overrelaxation method.

In Fig. 1 we compare our *bc* FSA results for the unrenormalized gluon propagator $D(p)$ calculated on a 44^4 lattice with those of the standard *fc* OR method obtained for an 80^4 lattice in Ref. [65]; all data produced for $\beta = 2.3$.[3] One can see that our *bc* FSA data points lie essentially below those of the *fc* OR method for momenta $|p| \lesssim 0.7$ GeV. Thus, we observe that the OR method with one gauge copy produces unreliable results for this range of momenta. Note that our lattice size is approximately twice as small as that in Ref. [65].

In the same figure we compare also with the *fc* SA results (no flips taken into account but much longer SA schedule applied) obtained for an 80^4 lattice in Ref. [66]. The data look consistent for the momentum region $|p| \gtrsim 0.3$ GeV. At smaller momenta, e.g., at $|p| \lesssim 0.3$ GeV the *fc* SA data points show the tendency to lie at somewhat lower values. The reason for this difference can be attributed to finite-volume effects (our lattice size is much smaller) or to uncertainties due to the lower statistics in [66]. In any case we confirm that the $Z(2)$ flips have the tendency to lower finite-size effects [60].

Let us define the Gribov copy sensitivity parameter $\Delta(p)$ as a normalized difference of the *fc* and *bc* gluon propagators

$$\Delta(p) = \frac{D^{fc}(p) - D^{bc}(p)}{D^{bc}(p)}, \quad (11)$$

where the numerator has been obtained by averaging the differences between *fc* SA and *bc* FSA propagators calculated for every configuration and normalized with the *bc* (averaged) propagator.

In Figs. 2–4 we show the momentum dependence of the Gribov copy sensitivity parameter $\Delta(p)$ for different lattices with physical sizes $aL \simeq 3$ fm, $aL \simeq 5$ fm and $aL \simeq 7.3$ fm, respectively.

Evidently, the Gribov copy effect is rather strong in the deep IR-region. It does not disappear with rising β, i.e. with the lattice spacing a becoming smaller. However, the effect decreases rapidly for rising momentum. Moreover, it is encouraging to see that the influence of Gribov copies for fixed momentum demonstrates clear tendency to decrease with increasing *physical* size aL. Thus, with our gauge fixing procedure we do not find any Gribov copy effect for momenta $p \gtrsim 0.6$ GeV on lattices with $aL \simeq 3$ fm, while on lattices with $aL \simeq 7.3$ fm the gluon propagator for all

---

[3]Only momenta $p \gtrsim 0.2$ GeV are shown for data from [65], note also that we are using a slightly different value for the lattice spacing than in [65].
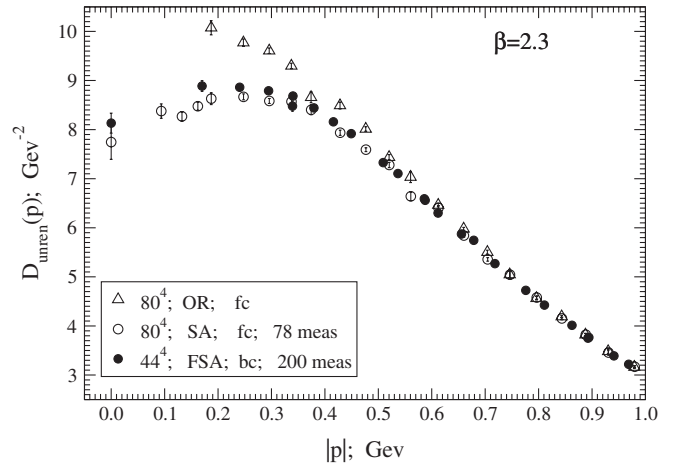

FIG. 1. Comparison of data obtained for *bc* FSA gauge fixing with those obtained with the standard *fc* OR—method and the *fc* SA algorithm (all for $\beta = 2.30$).

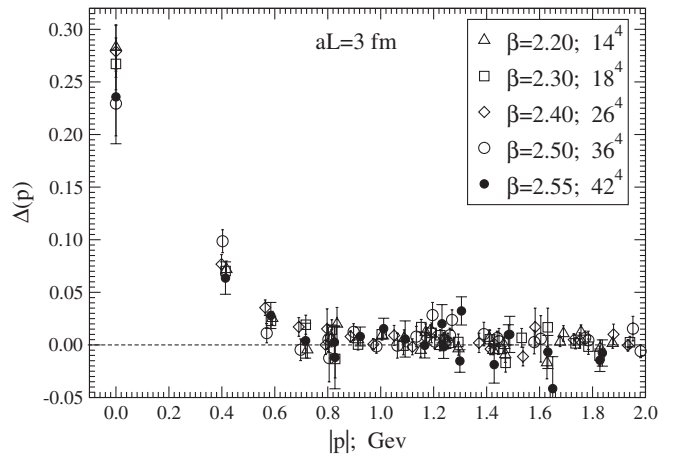
FIG. 2. The momentum dependence of the Gribov copy sensitivity parameter $\Delta(p)$ for various lattices with physical size $aL \simeq 3$ fm.
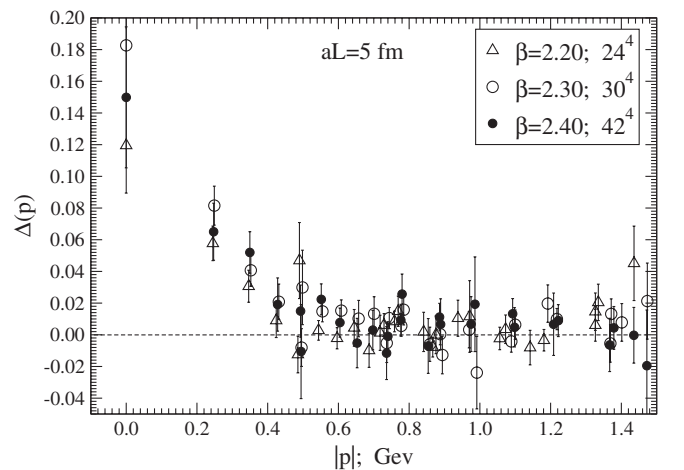

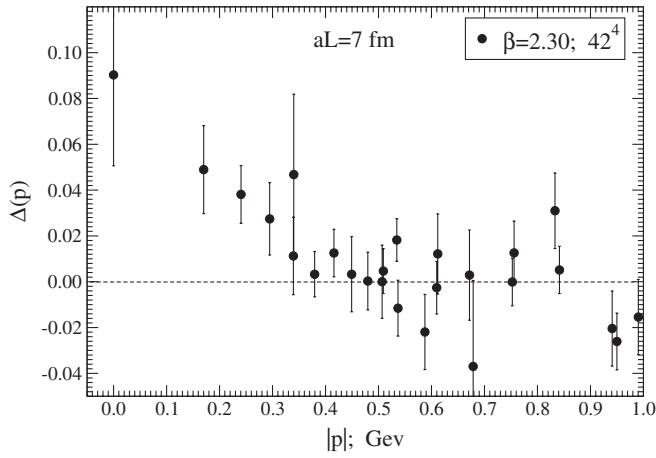FIG. 3. The momentum dependence of $\Delta(p)$ for various lattices with physical size $aL \simeq 5$ fm.

FIG. 4.   The momentum dependence of $\Delta(p)$ on a lattice with physical size $aL \simeq 7.3$ fm.

momenta $p \gtrsim 0.4$ Gev is free of Gribov copy effect. This tendency is in accordance with a conjecture by Zwanziger in [67] and was seen already for smaller lattice sizes in [68].

Let us finally note that the above observations are valid for our FSA gauge fixing method (employed with rather large number of gauge copies), which is proved to be much more powerful than, e.g., standard OR method. Of course, we cannot exclude that other even more efficient gauge fixing methods can be invented which might bring us even closer to the global extremum of the gauge functional. But we are convinced that this will not change the conclusions given here.

We would like to emphasize that the supposition to find the Gribov copies as close as possible to the global extremum of the Landau gauge functional differs substantially from the recent claim to study those Gribov copies maximally enhancing the infrared asymptotics of the ghost dressing function [47]. In as far these two different strategies really provide the different *decoupling* and *scaling* solutions, respectively, for the gluon and ghost propagators within the thermodynamic limit remains an interesting question.

V. NUMERICAL GLUON PROPAGATOR RESULTS

In order to suppress lattice artifacts from the beginning we followed Ref. [32] and selected the allowed lattice momenta as surviving the *cylinder cut*

$$\sum_{\mu} k_{\mu}^2 - \frac{1}{4}\left(\sum_{\mu} k_{\mu}\right)^2 \leq 3. \qquad (12)$$

Moreover, we have applied the "α-cut" [69] $p_{\mu} \leq (2/a)\alpha$ for every component, in order to keep close to a linear behavior of the lattice momenta $p_{\mu} = (2\pi k_{\mu})/(aL)$, $k_{\mu} \in (-L/2, L/2]$. We have chosen $\alpha = 0.5$. Obviously, this cut influences large momenta only.

We define the renormalized propagator $D_{\mathrm{ren}}(p)$ according to the momentum subtraction schemes (MOM) by

$$D_{\mathrm{ren}}(p, \mu) = Z_{\mathrm{ren}}(\mu, 1/a)D(p, 1/a) \qquad (13)$$

$$D_{\mathrm{ren}}(p = \mu) = 1/\mu^2. \qquad (14)$$

In practice we have fitted the bare propagators $D(p, 1/a)$ with an appropriate function (see Eq. (15) below) and then used the fits for renormalizing $D(p)$. But it has to be seen, that multiplicative renormalizability really holds in the nonperturbative regime. For this it is sufficient to prove, that ratios of the renormalized (or unrenormalized) propagators obtained from different cutoff values $1/a(\beta)$ will not depend on p at least within a certain momentum interval p_{min}, p_{max}, where p_{max} should be the maximal momentum surviving all the cuts applied.

In what follows the subtraction momentum has always been chosen to be $\mu = 2.2$ GeV. In Fig. 5 we show the momentum dependence of the renormalized gluon propagator $D_{\mathrm{ren}}(p)$ at comparatively large momenta ($|p| \gtrsim 1$ GeV) for five different lattice spacings but with (approximately) the same physical size $aL \simeq 3$ fm (for exact values see Table I). Evidently, in this momentum range the finite-spacing effects are rather small, at least for inverse bare coupling values $4/g_0^2 \equiv \beta > 2.2$.

In Fig. 6 for the same data set, we show the IR region only, whereas Fig. 7 presents the momentum dependence of the renormalized gluon dressing function $Z_{\mathrm{ren}}(p) = p^2 D_{\mathrm{ren}}(p)$ for the same lattice spacings as in Figs. 5 and 6. In both cases we see that there are quite strong deviations at least for $\beta = 2.2$. The early turnover of the gluon propagator $D_{\mathrm{ren}}(p)$ to an IR flattening is much less pronounced for higher β-values.

Our data for the larger volume of about $(5\ \mathrm{fm})^4$ demonstrate the behavior very similar to that of the volume $(3\ \mathrm{fm})^4$. Also in this case we find that the continuum limit
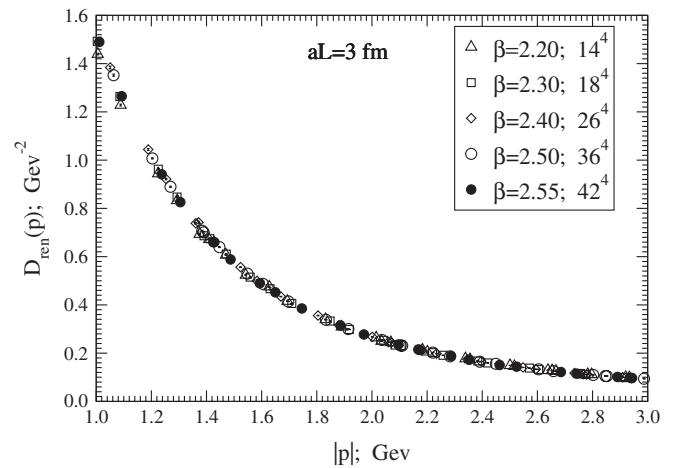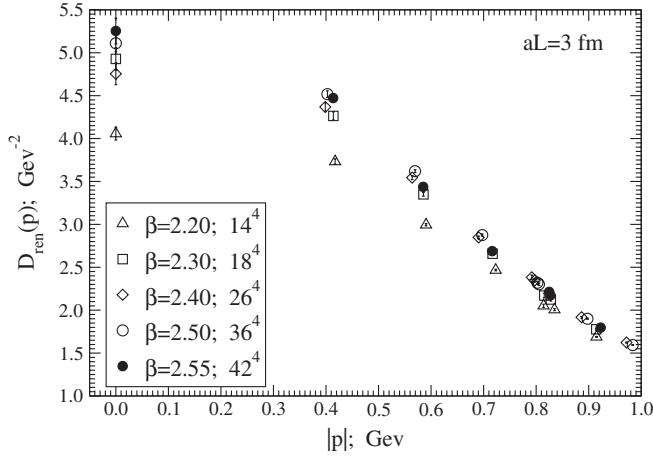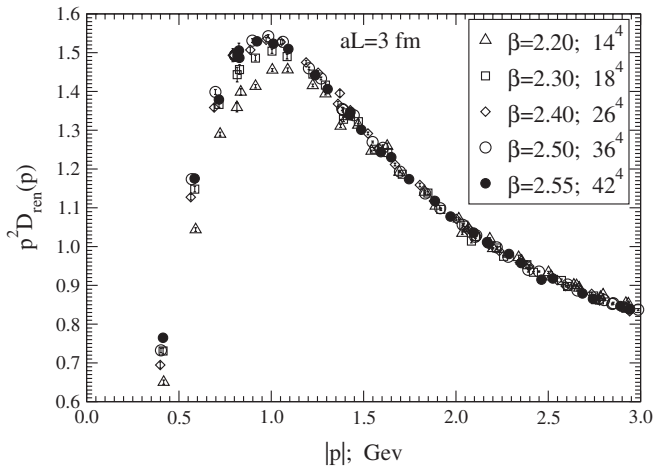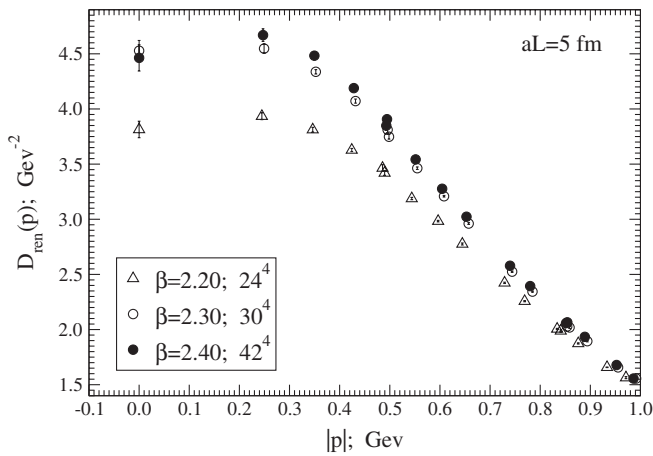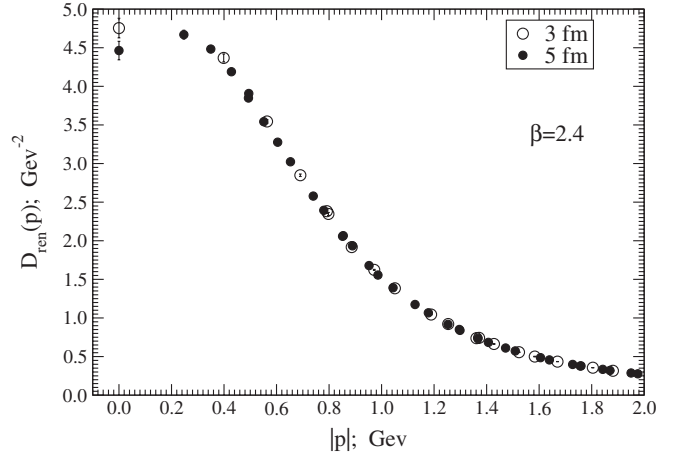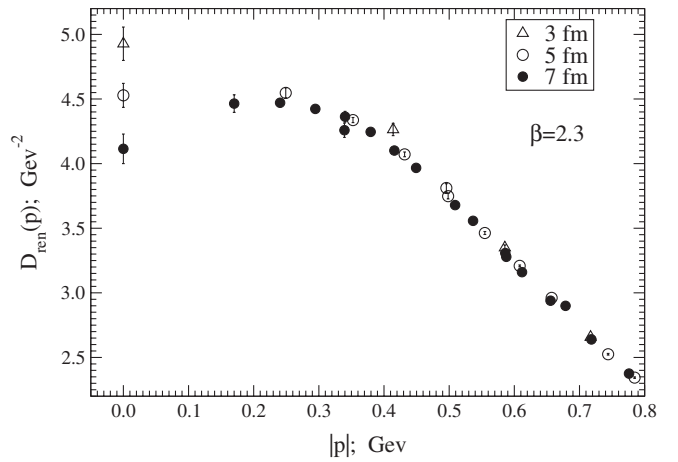

FIG. 5.   The momentum dependence of the gluon propagator $D_{\mathrm{ren}}(p)$ for five different lattice spacings and $|p| \gtrsim 1$ GeV. The physical linear box size is $aL \simeq 3$ fm.

FIG. 6. The same as in Fig. 5 but for $|p| \lesssim 1$ GeV.

FIG. 7. The momentum dependence of the renormalized dressing function $Z_{\mathrm{ren}}(p)$ for five different lattice spacings. The physical linear box size is $aL \simeq 3$ fm.

FIG. 8. The momentum dependence of the renormalized gluon propagator $D_{\mathrm{ren}}(p)$ for three different lattice spacings and $|p| \lesssim 1$ GeV. The physical linear box size is $aL \simeq 5$ fm.

FIG. 9. The momentum dependence of the renormalized gluon propagator $D_{\mathrm{ren}}(p)$ at fixed $\beta = 2.4$ for two different physical volumes.

is fastly reached for $\beta \gtrsim 2.3$ in the whole momentum range, whereas for $\beta = 2.2$ lattice artifact deviations occur, which become particularly strong in the infrared region $|p| \lesssim 1$ GeV. As an illustration, in Fig. 8 we show the IR region for three lattices for the volume $(5 \text{ fm})^4$.

In order to estimate finite-volume effects we compare our bc FSA data for the propagator $D_{\mathrm{ren}}(p)$ obtained for the same β-values but different aL. In Fig. 9 we show the momentum dependence of the renormalized gluon propagators $D_{\mathrm{ren}}(p)$ for two different physical sizes aL at $\beta = 2.4$, and in Fig. 10 $D_{\mathrm{ren}}(p)$ is presented for three different volumes at the somewhat stronger coupling $\beta = 2.3$. One can see that finite-volume effects are present only for the zero and minimal nonzero momenta and in the latter case they are rather small. Moreover, the IR flattening becomes visible only for the largest volume $aL \simeq 7$ fm.

FIG. 10. The momentum dependence of the renormalized gluon propagators $D_{\mathrm{ren}}(p)$ at fixed $\beta = 2.3$ for three different physical volumes.
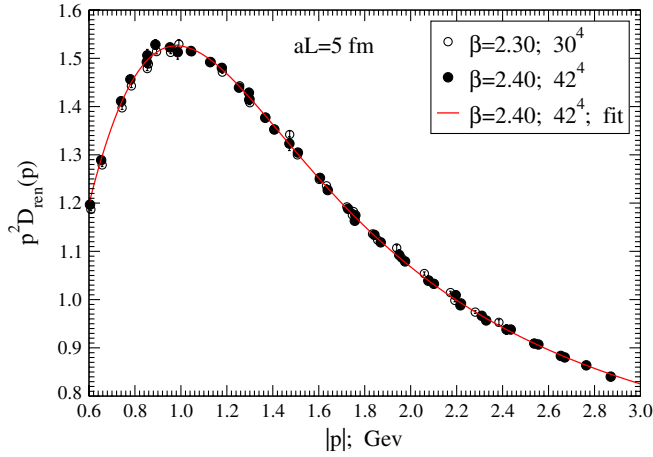
FIG. 11 (color online). The momentum dependence of the renormalized dressing function $Z_{\mathrm{ren}}(p)$ fitted at the smallest available lattice spacing compared with the data of coarser lattices. The linear box size is $aL \simeq 5$ fm.

Evidently, our data for the zero-momentum propagator $D_{\mathrm{ren}}(p = 0)$ show a clear tendency to decrease with increasing physical size aL. However, it remains difficult to speculate about the infinite-volume limit of $D_{\mathrm{ren}}(0)$.

In the literature one can find quite a few functional forms suggested to describe the gluon propagator in the IR-region, most of them of purely phenomenological origin, see e.g. [32]. For $\beta \geq 2.2$ we have fitted the momentum dependence of the gluon propagator with an ansatz describing a massive behavior in the infrared

$$D_{\mathrm{ren}}(p) = \frac{a_1}{p^2 + m^2} + \frac{a_2}{(p^2 + m^2)^2} + \frac{a_3}{(p^2 + m^2)^4}, \quad (15)$$

a_1, a_2, a_3 and m are fit parameters.

The fitting curves allow to compare quite easily the propagators obtained on different volumes. As an example, in Fig. 11 we show the fit results obtained for $p \gtrsim 0.6$ GeV for a physical volume $(5.0 \text{ fm})^4$. The fit parameters for all three volumes are provided in Table II.

TABLE II. Values of the fit parameters in physical units (with dimension $[a_1] = \text{GeV}^0$, $[a_2] = \text{GeV}^2$, $[a_3] = \text{GeV}^6$, $[m] = \text{GeV}$), and the corresponding χ^2_{df}.

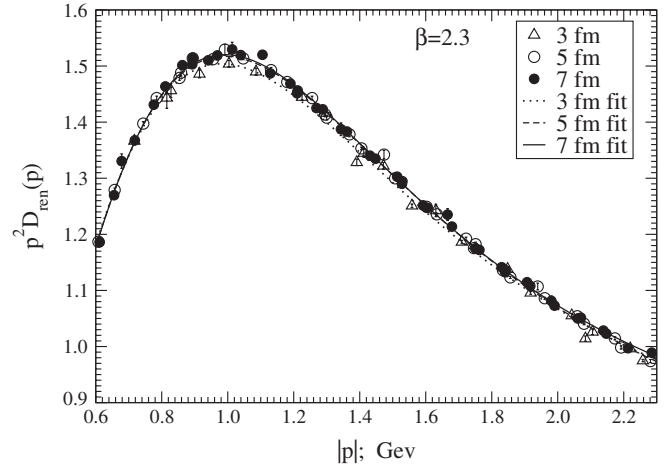| β	L	a_1	a_2	a_3	m	χ^2_{df}
2.20	14	0.62	4.58	49.5	1.38	5.0
2.30	18	0.61	4.03	54.5	1.37	3.8
2.40	26	0.56	4.31	50.8	1.35	1.5
2.50	36	0.55	4.30	39.5	1.30	1.5
2.55	42	0.56	4.34	45.0	1.34	1.2
2.20	24	1.02	1.33	128.4	1.53	3.6
2.30	30	0.59	4.19	61.0	1.39	2.6
2.40	42	0.55	4.39	53.9	1.37	0.5
2.30	44	0.67	3.65	72.2	1.41	1.6

FIG. 12. The renormalized dressing functions $Z_{\mathrm{ren}}(p)$ at $\beta = 2.3$. The data and the corresponding fits are shown for linear box sizes $aL \simeq 3, 5, 7$ fm.

In Fig. 12 we compare the data together with the corresponding fit curves obtained at $\beta = 2.3$ for the three physical volumes. We see that in the range shown $p \geq 0.6$ GeV finite-size effects are small at least for physical linear lattice sizes $aL \geq 5$ fm. Finally we check the multiplicative renormalizability by presenting the data for the gluon propagator ratio

$$R = D_{\mathrm{ren}}(p; \beta; L)/D_{\mathrm{ren}}^{\mathrm{fit}} \qquad (p; \beta = 2.55; L = 42) \quad (16)$$

in Fig. 13. The relative deviations are below 3% such that we can say multiplicative renormalizability is safe for $\beta \geq 2.4$ and for the momentum range $p \geq 0.6$ GeV. For $\beta = 2.3$ (not shown in the figure) the relative deviations are also below 3% for slightly shifted momentum range $p \geq 0.65$ GeV.
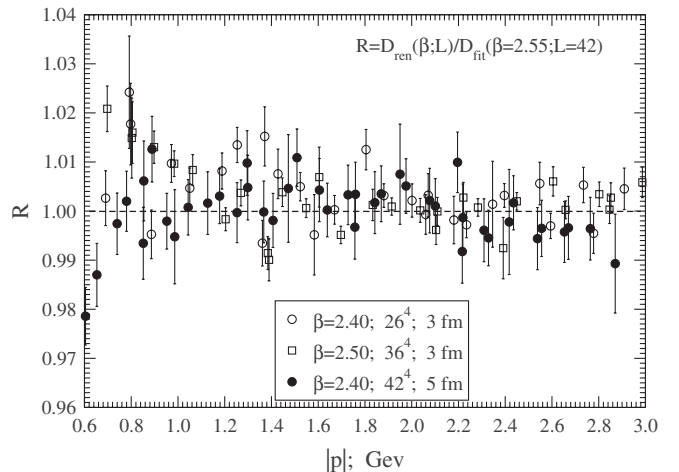

FIG. 13. The momentum dependence of the R-ratio for different β values and physical volumes.

VI. DEEP INFRARED REGION AND INFRARED MASS SCALE

In the previous section we discussed our fits of the propagator in the range $0.6 \lesssim p \lesssim 3$ GeV. An even more phenomenologically interesting range is the deep infrared region $|p| \lesssim 0.6$ GeV. As it was discussed in Sec. I the infrared mass scale is an important parameter for phenomenological analyses. Lattice results in principle can provide model independent information on this subject. Our results obtained in this region for $aL = 5$ fm and $\beta = 2.3$ and 2.4 exhibit only a weak dependence on the lattice spacing (see Fig. 8). Moreover, the finite-size dependence of $D(0)$ seems to be moderate at $\beta = 2.4$ (compare with Figs. 9 and 10). Therefore, let us speculate that our results for momenta below 0.6 GeV for $\beta = 2.4$ and $aL = 5$ fm are already close to the continuum and to the large-volume limit and that multiplicative renormalization can be assumed, too. Under these assumptions we have fitted our results at $p \lesssim 0.6$ GeV separately. We used two fitting functions to fit our data in this range of momenta. The first one is just the pole-type propagator providing an effective gluon mass scale m_g for $p \to 0$

$$D_{\text{pole}}(p) = \frac{A}{p^2 + m_g^2}. \qquad (17)$$

The other one is of the form of a Gaussian

$$D_{\text{gauss}}(p) = B e^{-(p-p_0)^2/m_{\text{IR}}^2}. \qquad (18)$$

A, m_g, B, p_0, m_{IR} are fit parameters. The results obtained for $\beta = 2.4$ and $aL = 5$ fm are compared in Fig. 14.

One can see that the pole-type momentum dependence given in Eq. (17) is not suitable for fitting the gluon propagator in the considered range of momenta. This is supported by the large value of the χ^2/ndf parameter value which was found to be about 14 if $p = 0$ is included and about 7 if this point is excluded. Therefore, the definition
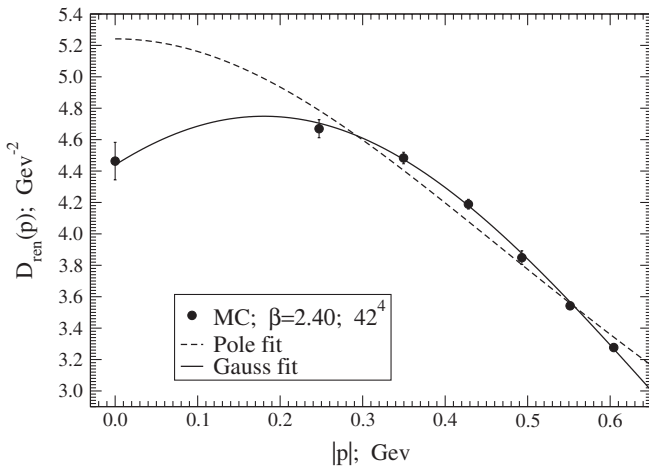

FIG. 14. The renormalized gluon propagator at $\beta = 2.4$ on $aL = 5$ fm lattice together with the infrared fits according to Eqs. (17) and (18).

of an effective gluon mass m_g via the tree-level Eq. (17) turns out to be problematic.

On the contrary, the Gaussian-type momentum dependence given in Eq. (18) nicely fits the data for the gluon propagator in the range $p \lesssim 0.6$ GeV with χ^2/ndf about 0.7 (0.5) with $p = 0$ included (excluded). Therefore, the Gaussian functional form allows to define an infrared (mass) scale m_{IR}. The numerical fit result is $m_{\text{IR}} = 0.69(3)$ MeV for $p = 0$ taken into account in the fit and 0.68(4) MeV, if $p = 0$ is ignored.

It is also interesting to note that our data suggest the existence of a maximum of the gluon propagator at a nonzero-momentum p_0. We have already observed this for $SU(2)$ in four dimensions in our previous work [44], where we studied the propagator on large lattices at $\beta = 2.2$, i.e. rather far from the scaling region. Our new results reported for $\beta = 2.3$ and 2.4 (see Figs. 9 and 10) show that the maximum seems to persist in the continuum limit. The mere existence of the maximum already contradicts a simple effective gluon mass prescription $\sim 1/(p^2 + m_g^2)$. With our fit function Eq. (18) we obtain $p_0 = 180(15)$ MeV, if the point $p = 0$ is included in the fit and 194(29) MeV, if $p = 0$ is ignored. Thus, the inclusion of $D(0)$ into the fit changes the value of p_0 only within error bars.

VII. CONCLUSIONS

In this work we investigated numerically the renormalized Landau gauge gluon propagator $D_{\text{ren}}(p)$ in the pure gauge $SU(2)$ lattice theory. The main goal of this study was to study the approach to the continuum limit, especially in the infrared region $|p| \lesssim 1$ GeV.

In order to disentangle finite-spacing from finite-volume effects we calculated the propagators on lattices with *physical* size aL equal approximately 3 fm at various β-values in the range of $\beta = 2.2, \ldots, 2.55$ and on lattices with $aL \approx 5$ fm for $\beta = 2.2, \ldots, 2.4$ (see Table I for details). Calculations were made also on $aL \approx 7.3$ fm lattices at $\beta = 2.3$. Our lattice volumes varied from $L^4 = 14^4$ to 44^4. For physical volumes $(aL)^4 \simeq (3$ fm$)^4$ and $(5$ fm$)^4$, we have checked the scaling behavior assuming the lattice spacing a to depend on β as determined from the string tension. The comparison of the renormalized propagators calculated for different physical volumes then allowed to estimate the influence of the finite (physical) volume in the infrared regime.

Special attention has been paid to the dependence on the choice of Gribov copies. In our previous papers [60,70] we have seen that the finite-volume behavior of the gluon propagator (and not only of the ghost propagator) is sensitive to the way how the Landau gauge is fixed. We found indications that by enlarging the gauge orbits by $Z(2)$-flip operations and by applying the simulated annealing method with consecutive overrelaxation ("FSA" algorithm) the volume dependence becomes suppressed.

However, our former investigations went immediately to largest accessible lattice volumes by employing coarse lattices ($\beta = 2.2$), such that the continuum limit remained to be studied.

Our findings can be summarized as follows.

(1) In the region $|p| \gtrsim 0.6$ GeV we observe very nice agreement between renormalized propagators $D_{\mathrm{ren}}(p)$ obtained for different lattices with $\beta \geq 2.4$. For larger momenta scaling holds for even smaller β values. In contrast, in the deep infrared region ($|p| \lesssim 0.6$ GeV) the scaling violation is quite strong, especially for $\beta = 2.2$. However, with increasing β finite-spacing effects rapidly decrease: our data seem to "converge" to some limiting curve of the renormalized propagator $D_{\mathrm{ren}}(p)$ (compare, e.g., propagators at $\beta = 2.2$ and $\beta = 2.55$), thus indicating the approach to the *continuum limit* in the fixed physical volume $(aL)^4$.

(2) Using our gauge fixing procedure we observed finite (physical) volume effects only for zero and minimal nonzero momenta. We made this observation for $\beta = 2.2$ in [44], here we confirm it for $\beta = 2.3$ and 2.4 and thus it can be extended to the continuum limit.

(3) In our previous papers [44,60] we calculated gluon propagators on various lattices at $\beta = 2.2$. We observed the appearance of a maximum at a nonzero value of the momentum p on lattices with comparatively large-volume ($aL \geq 6.7$ fm). Our new data obtained at larger β-values do confirm this observation. Fitting the propagator calculated at $\beta = 2.4$ by the fitting function Eq. (18) we obtained our best estimation for the position of this maximum as $p_0 = 180(15)$ MeV. This number might slightly change in the continuum limit. Also we observed that the zero-momentum gluon propagator $D(0)$ has a tendency to decrease with growing lattice size L. We did not try here to extrapolate its infinite-volume value.

(4) The effective gluon mass m_g has been employed as an important parameter in various phenomenological analyses. We fitted our results at $p \lesssim 0.6$ GeV using our data for the gluon propagator at $\beta = 2.4$ on lattices with $aL \approx 5$. It was found that the pole-type momentum dependence given by Eq. (17) does not provide an adequate description of our data at small momenta, which makes it problematic to define this parameter from the Landau gauge gluon propagator. On the contrary, a Gaussian-type behavior given by Eq. (18) fits the data nicely. It allows to define an alternative infrared (mass) scale $m_{\mathrm{IR}} = 0.69(3)$ GeV describing the approach to the infrared limit. Its consequences for phenomenological applications remain to be seen.

(5) We confirm that the Gribov copy influence is very strong in the deep infrared region. Comparing our *bc* FSA results calculated on a 44^4 lattice with those of the standard *fc* OR method obtained for an 80^4 lattice in Ref. [65] (see Fig. 1) we found that the OR method with one gauge copy produces unreliable results for momenta $|p| \lesssim 0.7$ GeV. We conclude that *fc* OR method should be applied exclusively to large-momentum studies.

Our FSA method provides systematically higher values of the gauge fixing functional as compared to the standard OR procedure. We studied the Gribov copy effect for this method as well, generating up to 80 gauge copies for every configuration. We found for fixed physical volume the Gribov copy sensitivity parameter $\Delta(p)$ only weakly to depend on the lattice spacing a. Therefore, the *quality* of the gauge fixing procedure in the study of gauge dependent observables remains important, at least, in the deep infrared.

At the same time the influence of Gribov copies demonstrates clear tendency to decrease for fixed momentum with increasing *physical* size aL. This tendency is in accordance with a conjecture by Zwanziger in [67] and was seen already for smaller lattice sizes in [68].

ACKNOWLEDGMENTS

[1] V. N. Gribov, Nucl. Phys. **B139**, 1 (1978).

[2] D. Zwanziger, Nucl. Phys. **B364**, 127 (1991).

[3] T. Kugo and I. Ojima, Prog. Theor. Phys. Suppl. **66**, 1 (1979).

[4] D. Zwanziger, Phys. Rev. D **65**, 094039 (2002).

[5] D. Zwanziger, arXiv:0904.2380.

[6] G. Parisi and R. Petronzio, Phys. Lett. B **94**, 51 (1980).

[7] J. H. Field, Phys. Rev. D **66**, 013013 (2002).

[8] A. A. Natale, arXiv:0910.5689.

[9] R. Alkofer and L. von Smekal, Phys. Rep. **353**, 281

(2001).

[10] R. Alkofer, Braz. J. Phys. **37**, 144 (2007).
[11] G. Eichmann, I. C. Cloet, R. Alkofer, A. Krassnigg, and C. D. Roberts, Phys. Rev. C **79**, 012202 (2009).
[12] K. G. Chetyrkin, Nucl. Phys. **B710**, 499 (2005).
[13] K. G. Chetyrkin and A. Maier, arXiv:0911.0594.
[14] A. Sternbeck, K. Maltman, L. von Smekal, A. Williams, E.-M. Ilgenfritz, and M. Müller-Preussker, Proc. Sci., LAT2007 (**2007**) 256.
[15] L. von Smekal, K. Maltman, and A. Sternbeck, Phys. Lett. B **681**, 336 (2009).
[16] L. von Smekal, R. Alkofer, and A. Hauck, Phys. Rev. Lett. **79**, 3591 (1997).
[17] L. von Smekal, A. Hauck, and R. Alkofer, Ann. Phys. (N.Y.) **267**, 1 (1998).
[18] R. Alkofer, C. S. Fischer, and L. von Smekal, Eur. Phys. J. A **17**, 773 (2003).
[19] C. S. Fischer and R. Alkofer, Phys. Lett. B **536**, 177 (2002).
[20] C. S. Fischer, R. Alkofer, and H. Reinhardt, Phys. Rev. D **65**, 094008 (2002).
[21] J. M. Pawlowski, D. F. Litim, S. Nedelko, and L. von Smekal, Phys. Rev. Lett. **93**, 152002 (2004).
[22] R. Alkofer, C. S. Fischer, and F. J. Llanes-Estrada, Phys. Lett. B **611**, 279 (2005).
[23] C. S. Fischer and J. M. Pawlowski, Phys. Rev. D **75**, 025012 (2007).
[24] P. Boucaud *et al.*, Eur. Phys. J. A **31**, 750 (2007).
[25] P. Boucaud *et al.*, J. High Energy Phys. 06 (2008) 012.
[26] P. Boucaud *et al.*, J. High Energy Phys. 06 (2008) 099.
[27] A. C. Aguilar, D. Binosi, and J. Papavassiliou, Phys. Rev. D **78**, 025010 (2008).
[28] C. S. Fischer, A. Maas, and J. M. Pawlowski, Ann. Phys. (N.Y.) **324**, 2408 (2009).
[29] J. Braun, H. Gies, and J. M. Pawlowski, Phys. Lett. B **684**, 262 (2010).
[30] H. Suman and K. Schilling, Phys. Lett. B **373**, 314 (1996).
[31] A. Cucchieri, Nucl. Phys. **B508**, 353 (1997).
[32] D. B. Leinweber, J. I. Skullerud, A. G. Williams, and C. Parrinello (UKQCD), Phys. Rev. D **60**, 094507 (1999).
[33] D. Becirevic *et al.*, Phys. Rev. D **60**, 094509 (1999).
[34] F. D. R. Bonnet, P. O. Bowman, D. B. Leinweber, and A. G. Williams, Phys. Rev. D **62**, 051501 (2000).
[35] F. D. R. Bonnet, P. O. Bowman, D. B. Leinweber, A. G. Williams, and J. M. Zanotti, Phys. Rev. D **64**, 034501 (2001).
[36] J. C. R. Bloch, A. Cucchieri, K. Langfeld, and T. Mendes, Nucl. Phys. B, Proc. Suppl. **119**, 736 (2003).
[37] J. C. R. Bloch, A. Cucchieri, K. Langfeld, and T. Mendes, Nucl. Phys. **B687**, 76 (2004).
[38] T. D. Bakeev, E.-M. Ilgenfritz, V. K. Mitrjushkin, and M. Müller-Preussker, Phys. Rev. D **69**, 074507 (2004).
[39] A. Sternbeck, E.-M. Ilgenfritz, M. Müller-Preussker, and A. Schiller, Phys. Rev. D **72**, 014507 (2005).
[40] P. O. Bowman *et al.*, Phys. Rev. D **76**, 094505 (2007).
[41] A. Cucchieri and T. Mendes, Proc. Sci., LAT2007 (**2007**) 297.
[42] A. Cucchieri and T. Mendes, Phys. Rev. Lett. **100**, 241601

(2008).

[43] A. Cucchieri and T. Mendes, Phys. Rev. D **78**, 094503 (2008).
[44] V. G. Bornyakov, V. K. Mitrjushkin, and M. Müller-Preussker, Phys. Rev. D **79**, 074504 (2009).
[45] I. L. Bogolubsky, E.-M. Ilgenfritz, M. Müller-Preussker, and A. Sternbeck, Phys. Lett. B **676**, 69 (2009).
[46] L. von Smekal, M. Ghiotti, and A. G. Williams, Phys. Rev. D **78**, 085016 (2008).
[47] A. Maas, arXiv:0907.5185.
[48] D. Dudal, S. P. Sorella, N. Vandersickel, and H. Verschelde, Phys. Rev. D **79**, 121701 (2009).
[49] D. Dudal, N. Vandersickel, H. Verschelde, and S. P. Sorella, arXiv:0911.0082.
[50] C. Parrinello and G. Jona-Lasinio, Phys. Lett. B **251**, 175 (1990).
[51] D. Zwanziger, Nucl. Phys. **B345**, 461 (1990).
[52] A. Nakamura and M. Plewnia, Phys. Lett. B **255**, 274 (1991).
[53] V. G. Bornyakov, V. K. Mitrjushkin, M. Müller-Preussker, and F. Pahl, Phys. Lett. B **317**, 596 (1993).
[54] V. K. Mitrjushkin, Phys. Lett. B **389**, 713 (1996).
[55] I. L. Bogolubsky, V. K. Mitrjushkin, M. Müller-Preussker, and P. Peter, Phys. Lett. B **458**, 102 (1999).
[56] C. S. Fischer, B. Gruter, and R. Alkofer, Ann. Phys. (N.Y.) **321**, 1918 (2006).
[57] C. S. Fischer, A. Maas, J. M. Pawlowski, and L. von Smekal, Ann. Phys. (N.Y.) **322**, 2916 (2007).
[58] G. S. Bali, V. Bornyakov, M. Müller-Preussker, and F. Pahl, Nucl. Phys. B, Proc. Suppl. **42**, 852 (1995).
[59] I. L. Bogolubsky, V. G. Bornyakov, G. Burgio, E.-M. Ilgenfritz, V. K. Mitrjushkin, M. Müller-Preussker, and P. Schemel, Proc. Sci., LAT2007 (**2007**) 318.
[60] I. L. Bogolubsky, V. G. Bornyakov, G. Burgio, E.-M. Ilgenfritz, V. K. Mitrjushkin, and M. Müller-Preussker, Phys. Rev. D **77**, 014504 (2008).
[61] J. E. Mandula and M. Ogilvie, Phys. Lett. B **185**, 127 (1987).
[62] J. Fingberg, U. M. Heller, and F. Karsch, Nucl. Phys. **B392**, 493 (1993).
[63] B. Lucini and M. Teper, J. High Energy Phys. 06 (2001) 050.
[64] P. Schemel, Diploma thesis, Humboldt University Berlin/ Germany, 2006.
[65] A. Sternbeck, L. von Smekal, D. B. Leinweber, and A. G. Williams, Proc. Sci., LAT2007 (**2007**) 340.
[66] I. L. Bogolubsky, E.-M. Ilgenfritz, M. Müller-Preussker, and A. Sternbeck, Proc. Sci., LAT2009 (**2009**) 237.
[67] D. Zwanziger, Phys. Rev. D **69**, 016002 (2004).
[68] I. L. Bogolubsky, G. Burgio, V. K. Mitrjushkin, and M. Müller-Preussker, Phys. Rev. D **74**, 034503 (2006).
[69] Y. Nakagawa, A. Voigt, E.-M. Ilgenfritz, M. Müller-Preussker, A. Nakamura, T. Saito, A. Sternbeck, and H. Toki, Phys. Rev. D **79**, 114504 (2009).
[70] I. L. Bogolubsky, V. G. Bornyakov, G. Burgio, E.-M. Ilgenfritz, V. K. Mitrjushkin, and M. Müller-Preussker, arXiv:0804.1250.